Zentrum für Technomathematik
Fachbereich 3 – Mathematik und Informatik

# Efficient methods in hyperthermia treatment planning

Torsten Köhler
Peter Maass
Peter Wust
Martin Seebass

Report 01–01

Berichte aus der Technomathematik

Report 01–01 Januar 2001

# Efficient methods in hyperthermia treatment planning

**Torsten Köhler†|| , Peter Maaß†, Peter Wust‡ and Martin Seebass§**

† Universität Bremen, Zentrum für Technomathematik, PF 33 04 40, 28334 Bremen, F.R.G.

‡ Humboldt-Universität Berlin, Charité, Campus Virchow–Klinikum, Augustenburger Platz 1, 13353 Berlin, F.R.G.

§ Konrad–Zuse–Zentrum für Informationstechnik, Takustr. 7, 14195 Berlin, F.R.G.

E-mail: koehler@math.uni-bremen.de

**Abstract.** The aim of this paper is to describe and analyse functionals which can be used for computing hyperthermia treatment plans. All these functionals have in common that they can be optimized by efficient numerical methods. These methods have been implemented and tested with realistic patient data from the Charité Berlin, Campus Virchow-Klinikum. The results obtained by these fast routines are comparable to those obtained by relatively expensive global optimization techniques. Thus the described methods are very promising for online optimization in a hybrid system for regional hyperthermia where a fast response to MR–based information is important.

Submitted to: *Phys. Med. Biol.*

|| To whom correspondence should be addressed

## 1. Introduction

Regional hyperthermia (RHT) is going to take a technological step in the next future. The basic idea is to heat up a deaply seated tumor region $\Omega$ to desired temparatures as complete as possible while keeping the temperatures in the surrounding healthy tissue $G \setminus \Omega$ below specified critical values. In case of achieving a good heat treatment the efficacy of a simultaneous or subsequent chemo- and/or radiotherapy regimen might be enhanced.

The energy deposition inducing the temperature increase is achieved with a set of $N$ radiowave antennas surrounding the patient. The latest generation of hyperthermia equipment uses up to $N = 24$ antennas, which are positioned on an elliptic cylinder in three rings and operate at the same frequency in a defined phase relation. The free parameters are the phase delays $\varphi_j$ with respect to a reference phase and amplitudes $a_j$ $(j = 1, \ldots, N)$ of the emitted radiowaves.

A basic hyperthermia treatment plan (for $N$ antennas) therefore consists of $N$ complex numbers $p_j = a_j \exp(-\mathrm{i}\varphi_j)$ which determine the power deposition pattern and the resulting temperature distribution in the body. More precisely the forward problem of computing the steady state temperature distribution inside the body $G$ for a given set of parameters $p = (p_1, \ldots, p_N)^{\mathrm{t}} \in \mathbb{C}^N$ can be splitted in two steps:

- computation of the resulting electric field distribution $E(x)$ inside the inhomogeneous body by solving Maxwell's equations,
- computation of the temperature distribution $T(x)$ by solving the bio-heat-transfer equation, assuming perfusion in every tissue point $x$ of $G$.

Now we can state the inverse or optimization problem of hyperthermia treatment planning in more detail. Let us assume that critical temperatures $T_{\mathrm{c}}(x)$ has been assigned by medical reasons for every point $x \in G \setminus \Omega$ in healthy tissues. Then we are looking for

$$\max_{p \in \mathbb{C}^N} T_{90} \quad \text{subject to} \quad T(x) \leq T_{\mathrm{c}}(x) \quad \forall x \in G \setminus \Omega \tag{1}$$

where $T_{90}$ is the temperature achieved by 90% of $x \in \Omega$. This is a high-dimensional nonlinear optimization problem in a Banach space formulation which requires substantial computational effort. Most of this paper deals with adequate simplifications of this functional which can be solved efficiently.

Recently a second generation of hyperthermia systems is going to get installed in some oncological centers. The above mentioned triple-ring applicator with 12 antenna pairs, i.e. 24 antennas, ist now commercially available as the so-called SIGMA-Eye applicator (BSD Medical Corp., Utah, USA). Simulation studies employing a global optimization routine formerly have demonstrated that this 24-antenna applicator can significantly improve the control of $SAR$-patterns ($SAR$: specific absorption rate) in comparison to the clinically used SIGMA-60 applicator (consisting of one ring of 4 antenna pairs, i.e. 8 antennas) (Wust *et al* 1996).

Modern hyperthermia systems are built in a hybrid technique, i.e. the RHT applicators operate in the field of view of a magnetic resonance tomograph (MRT). Online registration of temperature distributions (noninvasive thermography, see e.g. (Wloderczyk *et al* 1998, Wloderczyk *et al* 1999, Roemer 1995), can elucidate regions exceeding critical temperatures (typically $> 43,5°$C, so-called hot spots), and enables in conjunction with clinical informations (e.g. localized discomfort or other intolerances) a reformulation of the optimization problem in (1). The latter is performed by modifying perfusions and adapting weighting factors as described later in this paper. However, a fast and reliable solution of the inverse problem (1) will be required in real-time (preferably in seconds) during heat treatments under MR-monitoring by matching the adjustments to the individual clinical characteristics.

This paper deals with the development of efficient and flexible optimization strategies for regional radiofrequency hyperthermia which are useful for interactive online control. A global optimization method, optimizing suitable functionals (objective functions) by efficient search algorithms (e.g. used in (Wust *et al* 1996)), is utilized as a reference method. The first basic ideas for an elegant formulation of hyperthermia optimization problems as an eigenvalue-problem have been described in (Böhm *et al* 1993) and (Bardati *et al* 1995). A considerable generalization of this approach with respect to three-dimensional models, inclusion of temperature distribution, weight functions and time dependencies is outlined in the following.

## 2. Methods

First in subsection 2.1 the basic equations for $E$-field, power and temperature distribution are outlined. In the following we define functionals which are suitable to optimize the power deposition pattern (subsection 2.2) or the temperature distribution directly (subsection 2.3). The formulation of the optimization problem is performed in a way that requires the solution of a generalized eigenvalue problem. For the latter task efficient routines are available.

### *2.1. Basic mathematical models*

We assume $N$ antennas operating in a coherent mode at frequency $\omega$. The free parameters consist of $N$ complex amplitudes $p_j = a_j \exp(-\mathrm{i}\varphi_j)$, which are combined in the vector $p$. Each antenna generates an electric field $p_j E_j(x)$, where $E_j$ describes the normalized electric field of antenna $j$ alone, assuming $a_{i,j} = 0$ and a $50\,\Omega$ load for the other antennas $i \neq j$ . The relation between homogeneous and inhomogeneous media, given by Maxwell's equations, is included in the $E_j$'s. Integral equation methods (Wust *et al* 1999b), finite difference methods (Nadobny *et al* 1998) as well as finite element methods (Beck *et al* 1999), are employed to calculate $E_j(x)$. Various problems and controversies concerning the $E$-field calculation are discussed elswhere (Wust *et al* 1999b, Gellermann *et al* 1999).

The total electric field is then generated by a superposition of the basic electric fields $E_j$:

$$E(p)(x) \;=\; \sum_{j=1}^{N} p_j \; E_j(x) \quad . \tag{2}$$

A relevant quantity for hyperthermia treatment is not the electric field itself but rather the absorbed power ($ARD$, absorbed rate density, in $\mathrm{W/dm^3}$), which also depends on the electric conductivity $\sigma$ (in S/m):

$$ARD(p)(x) \;=\; \sigma(x) \; |E(x)|^2 \; .$$

First mathematical approaches in hyperthermia treatment planning focussed on optimizing the $ARD$ distribution, see e.g. (Böhm *et al* 1993). We will describe this approach in more detail in section 2.2.

The ultimate aim of hyperthermia treatment plannig is to optimize the resulting temperature distribution. So far no complete and efficient model exists, which incorporates all aspects of the heat transfer (diffusion, perfusion, large vessels, whole whessel free temperature regulation etc.). However a standard simplified model, the stationary bio-heat-transfer-equation, governs major aspects and produces results which agree sufficiently with reality. More precisely its solution determines the increase in temperature, $T_{\mathrm{hyp}}(x)$, achieved by a given $ARD$-distribution:

$$\mathrm{div}(\kappa \, \mathrm{grad} T_{\mathrm{hyp}}) \;-\; cWT_{\mathrm{hyp}} + ARD \;=\; 0 \; . \tag{3}$$

Here $c$ combines several quantities describing the material properties of the blood flow, $W(x)$ models the local perfusion, $\kappa(x)$ denotes thermal conductivity.

Thus the computation of a temperature distribution essentially consists of two steps. Given a control vector $p$ one has to compute the $E_j$ by solving Maxwells equations (see above) and to compute $T$ by solving (3), exploiting the fact, that a slightly more complicated superposition principle analogous to (2) holds for $T_{\mathrm{hyp}}$. Equation (3) is solved very efficiently using an adaptive finite-element code (Bornemann *et al* 1993, Deuflhard *et al* 1989). The inverse or optimization problem is formulated in (1).

### *2.2. Functionals for hyperthermia treatment planning*

As already stated, optimizing the functional in (1) requires to solve a high-dimensional, non-linear optimization problem. This approach is not suitable for computer-aided optimizations in real time.

One specific optimization criterion was introduced in (Böhm *et al* 1993). This approach starts with a functional which compares the absorbed energy in the tumor region $\Omega$ with the absorbed energy in the healthy tissues $G \setminus \Omega$:

$$\max_{p \in \mathbb{C}^N, \|p\|=1} \frac{\int\limits_{\Omega} \sigma(x)|E(x)|^2 \, \mathrm{d}x}{\int\limits_{G \setminus \Omega} \sigma(x)|E(x)|^2 \, \mathrm{d}x} \;=\; \max_{p \in \mathbb{C}^N, \|p\|=1} \frac{||E||_{L^2(\Omega,\sigma)}}{||E||_{L^2(G\setminus\Omega,\sigma)}} \quad . \tag{4}$$

This functional differs substantially from (1). However, from a mathematical point of view, the advantage of this new functional lies in its Hilbert space structure, which allows an efficient computation. Using (2) this functional is equivalent to

$$\max_{p\in\mathbb{C}^N,\|p\|=1} \frac{\langle p, Ap\rangle_{\mathbb{C}^N}}{\langle p, Bp\rangle_{\mathbb{C}^N}} \tag{5}$$

with $N \times N$ matrices $A, B$:

$$\begin{aligned} A_{ij} &= \int_{\Omega} \sigma(x) E_i(x) \overline{E_j(x)}\, \mathrm{d}x \\ B_{ij} &= \int_{G\setminus\Omega} \sigma(x) E_i(x) \overline{E_j(x)}\, \mathrm{d}x\ . \end{aligned} \tag{6}$$

This problem is solved by the normalized eigenvector corresponding to the largest generalized eigenvalue of

$$Ap = \lambda Bp\ . \tag{7}$$

The normalized largest eigenvector only gives the relationship between the different antenna parameters $p_j$. Hence, the final treatment plan is achieved by multiplying $p$ with an additional amplitude factor $a$, s.t. all restrictions in the healthy tissue are met.

In its original form this elegant approach was realized in a 2D setting. A generalization to higher dimensions is easily performed, but has several additional severe drawbacks:

(i) averaging over $G \setminus \Omega$ gives little weight to overheated areas of small extension in the healthy tissue, i.e. the resulting hyperthermia treatment plan can produce pronounced hot spots,

(ii) the approach is limited to optimize the $ARD$ distribution, i.e. the influence of the heat transport with respect to the temperature distribution is neglected.

The main purpose of this paper is to find a functional, which has the same structure as (4) but which better models clinical demands. I.e. we want to keep the efficient way of maximizing the resulting functional by a generalized eigenvalue problem.

Of course we would like to compare the results of our optimization procedure with the global optimum obtained by (1). However this functional is time-consuming to maximize. Hence, we use as reference the results obtained by a method described in (Lang *et al* 1997). The authors solve

$$\min_{p\in\mathbb{C}^N} \left\{ \int_{\Omega} f_1(x)\, \mathrm{d}x + v_2 \int_{G\setminus\Omega} f_2(x)\, \mathrm{d}x + v_3 \int_{G\setminus\Omega} f_3(x)\, \mathrm{d}x \right\} \tag{8}$$

with

$$f_1(x) = \begin{cases} (43 - T(x))^2 & \text{for } T(x) < 43^\circ\mathrm{C} \\ 0 & \text{otherwise,} \end{cases}$$

$$f_2(x) = \begin{cases} (T(x) - 42)^2 & \text{for } T(x) > 42°\text{C} \\ \\ 0 & \text{otherwise,} \end{cases}$$

$$f_3(x) = \begin{cases} (T(x) - T_c(x) - \varepsilon)^2 & \text{for } T(x) > T_c(x) - \varepsilon \\ \\ 0 & \text{otherwise,} \end{cases}$$

(with weight factors $v_1$ and $v_2$ for the corresponding terms) by an iterative method (damped Gauss-Newton method). This approach is a compromise between numerical efficiency and medical/clinical demands. We would like to stress, that approximating the global maximum of this functional can be done with reasonable numerical effort, but even a single step of the Gauss-Newton-iteration requires substantially more computation time then maximizing the functional (4) by solving (7) as described.

### *2.3. Efficient functionals for optimizing temperature distribution*

Again, we start with the basic functional (4). We will discuss various improvements of this functional leading to a clinically relevant and practical methodology for computing hyperthermia treatment plans. All of these functionals have the same structure as (4), hence they can be maximized by the simple eigenvalue computation. More specifically, we will follow two ideas:

- Temperature optimization: we introduce a functional, which allows to incorporate the temperature solution of the bio-heat-equation in a suitable Hilbert space functional,
- Generation of weight functions: theory offers the possibility of introducing suitable weight functions which can be used to consider particular attributes of the patient.

In section 2.2 we have described the method from (Böhm *et al* 1993) for optimizing the *ARD*-distribution

$$ARD(x) \;=\; \sigma(x)|E(x)|^2 \;=\; \sum_{i,j=1}^{N} p_i \overline{p}_j \sigma(x) E_i(x) E_j(x) \;.$$

In a first attempt we have experimented with functionals like (4), where the $L^2$-norm has been replaced by more general Sobolev norms of order $s > 0$ . This change was done in order to give more importance to localized structures with large derivatives like hot spots. The success of this approach was limited because the electric field $E$ also exhibits dicontinuities at every boundary between organs, bones, muscles etc., thus not only hot spots are weighted by using those norms. Moreover optimizing *ARD* instead of $T$ is often not reflecting clinical conditions, in particular if we are not considering any kind of heat transport.

So we turn to optimizing the temperature distribution itself. The main problem is to find adequate function spaces and functionals, which also allow an optimization

by a generalized eigenvalue problem. The temperature $T(x)$, which is finally reached by the hyperthermia treatment plan $p$, has two components: the basal temperature $T_{\text{bas}}$, which describes the temperature prior to the treatment, and $T_{\text{hyp}}$, the temperature increase due to $p$ and the related $ARD$-distribution. Thus for each $x \in G$ we have $T(x) = T_{\text{bas}}(x) + T_{\text{hyp}}(x)$ . The quantity $T_{\text{hyp}}$ is computed by solving the bio-heat-transfer equation (3), which describes a linear dependence of $T_{\text{hyp}}$ on $ARD$. So we have

$$T_{\text{hyp}}(ARD)(x) \;=\; \sum_{i,j=1}^{N} p_i \overline{p}_j T_{\text{hyp}}(\sigma E_i \overline{E}_j)(x) \;=\; \langle p, M(x)p \rangle \;,$$

where the coefficients of the matrix $M(x) = (M(x))_{ij})_{i,j=1}^{N}$ are the solutions of (3) with $ARD(x) = \sigma(x) E_i(x) \overline{E}_j(x)$. Hence, we restrict ourselves to optimize the increase in temperature $T_{\text{hyp}}$ in an $L^1$-setting. This is reasonable, because the basal temperature is rather homogeneous in the relevant interior of the body. We define

$$\max_{p \in \mathbb{C}^N, \|p\|=1} \frac{\int\limits_{\Omega} T_{\text{hyp}}(x)\, \mathrm{d}x}{\int\limits_{G \setminus \Omega} T_{\text{hyp}}(x)\, \mathrm{d}x} \;. \tag{9}$$

The functional (9) again is maximized by solving a generalized eigenvalue problem as stated in (7), where $A, B$ now are $N \times N$ matrices with

$$A_{ij} = \int\limits_{\Omega} M_{ij}(x)\, \mathrm{d}x \;,\; B_{ij} = \int\limits_{G \setminus \Omega} M_{ij}(x)\, \mathrm{d}x \;.$$

For more details see (Köhler 1999).

Significant improvements could be achieved by introducing suitable weight functions $w$. For this purpose we modify (9) to

$$\max_{p \in \mathbb{C}^N, \|p\|=1} \frac{\int\limits_{\Omega} T_{\text{hyp}}(x)\, w(x)\, \mathrm{d}x}{\int\limits_{G \setminus \Omega} T_{\text{hyp}}(x)\, w(x)\, \mathrm{d}x} \;, \tag{10}$$

which leads to matrizes $A$ and $B$ where the integrands of the elements have changed to $M_{ij}(x)\, w(x)$.

The main advantage of the latter approach in connection with a efficient eigenvalue optimization is its adaptiveness: starting with a preliminary weight function one obtains a temperature distribution, which might exhibit hot spots. This information can be used to formulate an adapted weight function for a second optimization step.

## 3. Results

### *3.1. The steady state case*

In the following we outline some results obtained with these different functionals. The treatment plan "sync" refers to a standard adjustment typically utilized if no optimization is available. Here constant $p$ with $p_i = p_j$ for $i, j = 1, \ldots, N$ was used.

**Table 1.** Results for optimizing the temperature distribution with different functionals. $T_{90}$ is the temperature achieved or exceeded by 90% of the target (near the minimum temperature), $T_{\text{mean}}$ is the averaged temperature and $V_{42}$ the percentage of the target with 42°C or more.

| antennas control | patient 1 | | | patient 2 | | |
|---|---|---|---|---|---|---|
| | $T_{90}$ | $T_{\text{mean}}$ | $V_{42}$ | $T_{90}$ | $T_{\text{mean}}$ | $V_{42}$ |
| "sync" | 39.09°C | 40.33°C | 3.48% | 38.48°C | 39.89°C | 2.96% |
| "$ARD - L^2$" | 39.15°C | 41.08°C | 30.13% | 38.48°C | 39.71°C | 0.00% |
| "$T_{\text{hyp}}$" | 39.43°C | 41.39°C | 35.51% | 38.28°C | 39.43°C | 0.00% |
| "$T_{\text{hyp}} w_{\text{sr}}$" | 39.52°C | 41.62°C | 41.71% | 40.23°C | 41.99°C | 51.07% |
| "$T_{\text{hyp}} w_{\text{sr}}^{\text{adapt}}$" | 39.78°C | 41.43°C | 34.94% | 40.51°C | 42.50°C | 64.42% |

"$ARD - L^2$" is obtained with the method of (Böhm *et al* 1993) as described in section 2.2. The result "$T_{\text{hyp}}$" is obtained with the (unweighted) functional (9). The values for "$T_{\text{hyp}} w_{\text{sr}}$" are caused by a control computed through a one-step-computation, using a weight function which can further differentiate between tissues or regions. Finally "$T_{\text{hyp}} w_{\text{sr}}^{\text{adapt}}$" stands for a control based on the adaptive strategy as described above.

Calculations have been done for two patients of the Charité Berlin, Campus Virchow-Klinikum: at first a female patient with a cervical carcinoma recurrence (patient 1), and secondly a male patient with a rectum carcinoma (patient 2). Initially, patient data were obtained on finite element grids to calculate field and temperature. For an efficient implementation of our techniques all these data have been interpolated to regular grids.

Table 1 displays three different quality measures for each of the hyperthermia treatment plans, normalized to a fixed total power. The index temperature $T_{90}$ (see legend of table 1) is accepted as most powerful predictor of the heat treatments quality among clinicians (which is derived from various clinical data, see e.g. (Rau *et al* 2000)).

Figures 1 and 2 display temperature distribution in a representative cross section and longitudinal section of patient 1 and 2, respectively, for different optimization strategies.

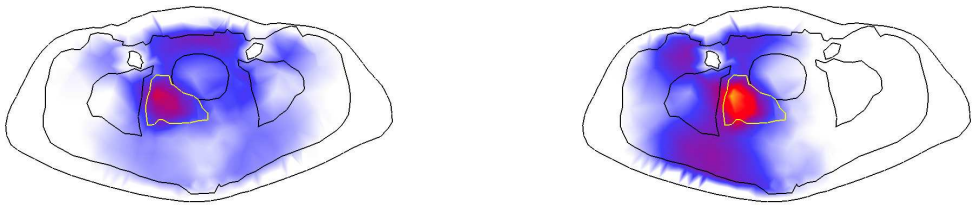

**Figure 1.** Temperature distributions on a cross section of patient 1 for the functionals "sync" (left) and "$ARD - L^2$" to illustrate small benefit obtained following the approach of (Böhm *et al* 1993).

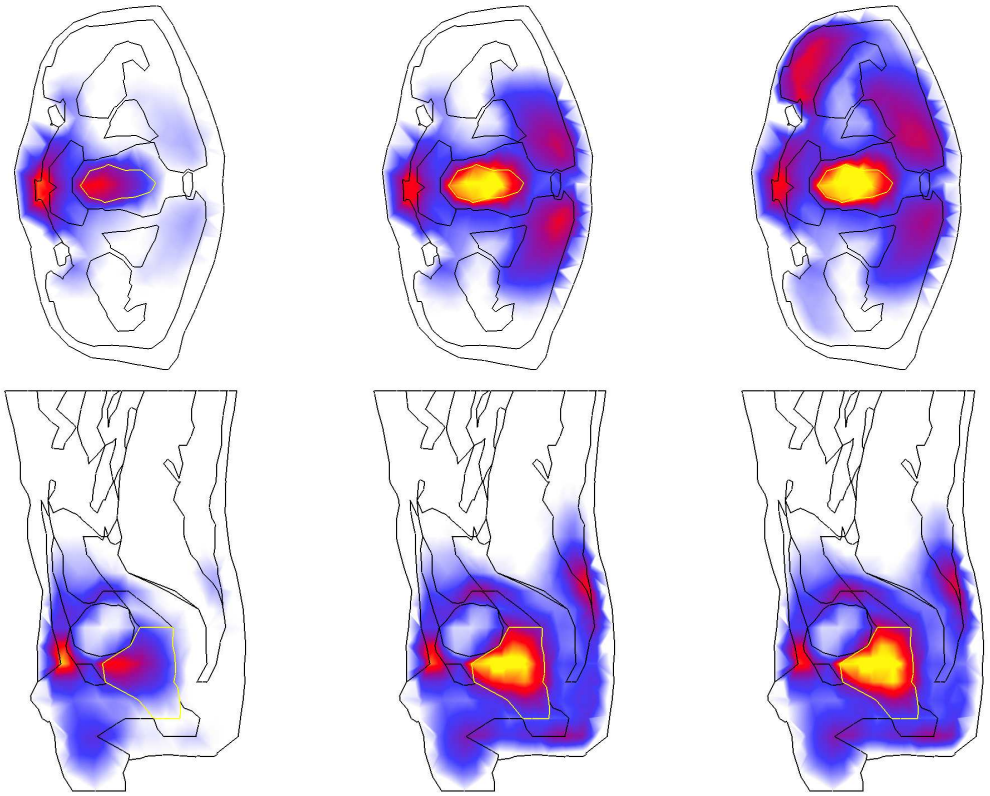

**Figure 2.** Temperature distributions on a cross section and longitudinal section of patient 2 for different functionals: "sync" (left), "$T_{\mathrm{hyp}} w_{\mathrm{sr}}^{\mathrm{adapt}}$" (center) and the result obtained by global optimization according to (Lang *et al* 1997) (right).

### *3.2. Modelling time-dependency*

So far the objective of our optimization is attributed to a single set of phases and power amplitudes $p$ in the steady state. However, this approach neglects the dynamic process of how the temperature increases from its original temperature $T_{\mathrm{bas}}(x)$ to the steady state temperature $T(x) = T_{\mathrm{bas}}(x) + T_{\mathrm{hyp}}(x)$. Modelling the time-dependency opens new directions for optimizing hyperthermia treatment plans. By following the time evolution of $T(x)$ and switching over the power deposition pattern before reaching a critical temperature value we can originally select adjustments which exhibit hot spots in their steady states. Lets assume a set of hyperthermia treatment plans, which in their steady states exhibit hot spots in different locations. This allows to adjust higher power amplitudes for these plans if we control the heating process in time and switch between these plans accordingly.

In order to put this in a mathematical framework we need a model as well as optimality criteria for the switching points.

Of course, a heuristic approach of this sort is used in clinical reality already. A typical hyperthermia treatment session lasts approximately 75-90 min. and the medical supervisor modifies the original $p$ according to the patients reactions. Our aim is to describe and implement some basic ideas for a strict mathematical optimization, which

can be utilized in a systematic way during a heat treatment.

Therefore, we assume a reasonable temporal transition between two steady-state temperature distributions from $T^{(1)}_{\text{hyp}}$ to $T^{(2)}_{\text{hyp}}$ according to Newtons cooling law, which leads to

$$T(x,t) \;=\; T_{\text{bas}}(x) \;+\; T^{(1)}_{\text{hyp}}(x) + \left(T^{(2)}_{\text{hyp}}(x) - T^{(1)}_{\text{hyp}}(x)\right)\left(1 - \exp(-\xi(x)t)\right)$$

(for further details see (Köhler 1999)). The exponent $\xi(x)$ varies locally in reality, especially in dependency on the tissue. However, in good approximation we can choose a medium and constant value $\xi(x) = 0.5$ .

Figure 3 shows the temperature-time-curve at a fixed point $x$ for a combination of antennas controls $p^{(1)}$ and $p^{(2)}$. On the left a combination of treatment plans were $p^{(2)}$ achieves a higher $T_{\text{hyp}}$ than $p^{(1)}$, on the right the opposit, which leads to cooling in position $x$ after switching over, is shown.

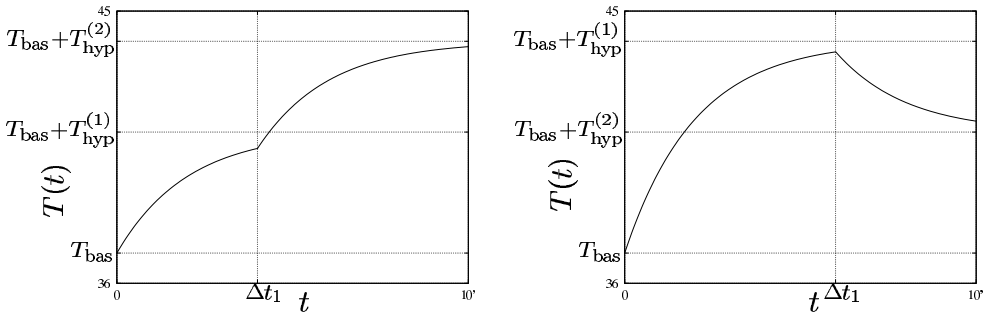


**Figure 3.** Heating/cooling profile in a certain point $x$ for a combination of two hyperthermia treatment plans.

In the following we describe the results obtained by combining two power deposition patterns $p^{(1)}$ and $p^{(2)}$. The weight function $w$ used in the computation of $p^{(2)}$ has been defined adaptively in dependency on the temperature distribution achieved with $p^{(1)}$ by choosing rather high weight factors in normal tissues, where high temperatures are achieved in the steady state sense. Here, one important optimality strategy is to enforce the controls to differ sufficiently with respect to the localization of arising hot spots. Moreover, we have to specify the duration $\Delta t_1$ and $\Delta t_2$ for each treatment plan. Due to our simple but realistic heating model, this low-dimensional optimization problem can be solved by a direct method, for details and implementational issues see (Köhler 1999).

In Table 2 for clearity we repeat some results starting from the method introduced in (Böhm *et al* 1993), continued by the best steady state solution (which was "$T_{\text{hyp}} w^{\text{adapt}}_{\text{sr}}$") for comparison with the descriptors of an average temperature distribution caused by a combination of two suitable controls as described above ("comb"). Finally for comparison we have listed the $T$-descriptors achieved with the global optimization of the functional (8).

Tables 1 and 2 demonstrate, that the temperatures in the target (tumor) can be increased remarkably by stepwise utilization of our optimization methods. Combining

**Table 2.** Some more optimization results, combined with two examples from Table 1 for comparison.

| antennas control | patient 1 | | | patient 2 | | |
|---|---|---|---|---|---|---|
| | $T_{90}$ | $T_{\mathrm{mean}}$ | $V_{42}$ | $T_{90}$ | $T_{\mathrm{mean}}$ | $V_{42}$ |
| "$ARD - L^2$" | 39.15°C | 41.08°C | 30.13% | 38.48°C | 39.71°C | 0.00% |
| "$T_{\mathrm{hyp}} w_{\mathrm{sr}}^{\mathrm{adapt}}$" | 39.78°C | 41.43°C | 34.94% | 40.51°C | 42.50°C | 64.42% |
| "comb" | 39.81°C | 41.46°C | 35.80% | 40.57°C | 42.63°C | 65.85% |
| "global" | 39.83°C | 41.53°C | 37.85% | 40.66°C | 42.74°C | 69.79 % |

just two antenna controls employing the efficient procedure sketched above, for both examples we achieved the best improvement. We would like to state that - within the accuracy of the used mathematical models - the latter method gives results, which are comparable with those obtained by the comparatively expensive global optimization.

## 4. Discussion

The next generation of RF-applicators (Sigma-Eye applicator) will require hyperthermia treatment planning, because the number of adjustable parameters (11 relative phases, 11 relative amplitudes) is much too high to find the "best adjustment" by intuition or trial and error (see (Wust *et al* 1996)). Treatment planning systems are now at a stage of clinical practicability, and a preliminary verification has also been performed (Gellermann *et al* 1999).

In particular, antenna models are available employing the FDTD-method or FE-method to describe the $E$-field in the water bolus quite accurate for the Sigma-60 applicator (Wust *et al* 1999a) and as well for the Sigma-Eye applicator (data to be published). Even though, a quite pronounced sensitivity from the patient model for the $E$-field ($SAR$-pattern) in the interior of the body is known (details of the segmentiation, grid, numerical method) (Gellermann *et al* 1999, Wust *et al* 1999b), accumulation of further experimental and clinical data will probably enable a valid patient-specific prediction of the power deposition pattern. Therefore, the forward problem until the level of $E(x)$ appears manageable.

On a weaker basis stands the numerical calculation of the temperature distribution (from the bioheat-transfer equation), mostly because of the variable tissue/tumour perfusion that is considerably influencing the temperature. The basic problem is that the perfusion under hyperthermia conditions is not well known, and furthermore can vary during heat treatments (e.g. because of local and systemic thermoregulatory process). Solutions of the inverse problem depend even more sensitively on numerous parameters, including the objective function itself, and especially the assumed perfusions and other details of the input. Clearly, all uncertainties of the prior planning process (patient model, $E$-field calculation, temperature calculation), and in addition individual variations such as positioning errors, shifts of organs and tissues thermoregulation,

systemic influences, intolerances etc. are accumulating. Therefore, in clinical use a continuous online adaptation of the optimization procedure according to the individual situation, i.e. during the heat treatment, appears obligatory.

A hybrid system is designed to deliver online information in order to adjust the optimization process:

- Registration of temperature distribution during heating-up after switch-on of power (i.e. delivering information about the gradient of temperature rise) can characterize the $SAR$-distribution in vivo.
- Registration of temperature distribution during steady state can characterize perfusion, and furthermore localize hot spots (which might or might not be predicted by the $SAR$-distribution prior determined). In addition, other methods to measure perfusion patterns are available in the MRI, e.g. utilizing contrast media bolus or other dedicated sequences.
- Individual intolerances might be found, reduced perfusion postsurgically or temperature-dependent sensations of any kind.

The optimization method described in this paper, especially the strategy to maximize the functional in (10), is in particular suitable to utilize the data from the hybrid system. The following CPU times are given for a Silicon Graphics Indigo 2 with 250 MHz MIPS and 192 MB RAM:

a) For a reclassified perfusion case (estimated form MRI) a computation of $M(x)_{ij}$ to determine $T_{\mathrm{hyp}}(x)$ according to (9) needs 6.5 s for 4 channels $(i,j = 1, \ldots, 4)$, and consequently 58.8 s for 12 channels $(i,j = 1, \ldots, 12)$ .

b) An adaptation of weighting factors needs 2 s for 4 channels and 18 s for 12 channels to recompute the matrices like in (10) (multiplying the integrand with $w(x)$) for solution of a generalized eigenvalue problem.

c) The solution of a generalized eigenvalue problem itself is performed very rapidly, i.e. in 0.1 s for 4 and less than 1 s for 12 channels, respectively.

The result of such an optimization process is an improved set of control parameters $p_j$ $(j = 1, \ldots, 4 \quad \text{or} \quad 1, \ldots, 12)$ of phases and amplitudes. Other functionals, like in (4), are also useful, e.g. if a change of conductivity $\sigma(x)$ is registered and considered ex posteriori.

The computation time for a completely updated optimization of the Sigma-Eye applicator (12 channels) is clinically feasible ($\ll 80$ s), and further reduction is expected with evolving computer technology (at least a factor 10). A considerable flexibility is available to customize the control parameters to changes in conductivity, perfusions, and individual intolerances of the patient. Therefore, the developed eigenvalue approach is especially useful for online optimization in a hybrid RHT-system.

## Acknowledgments

This work has been supported in parts by the Deutsche Forschungsgemeinschaft (DFG) (SFB 273, GraKo 331) and BMBF (grant MA7POT-6).

## References

Bardati F, Borrani A, Gerardino A and Lovisolo G.A. *SAR* Optimization in a Phased Array Radiofrequency Hyperthermia System 1995 *IEEE Trans. on Biomed. Eng.* **42** 1201–1207

Beck R, Deuflhard P, Hege H C, Seebass M and Stalling D 1997 Numerical Algorithms and Visualization in Medical Treatment Planning *Visualization and Mathematics*, ed Hege H C, Poltier K (Berlin) 303–325

Beck R, Deuflhard P, Hiptmair R, Hoppe R and Wohlmuth B 1999 Adaptive Multilevel Methods for Edge Element Discretizations of Maxwell's Equations *Surveys on Mathematics for Industry* **8** 271–312.

Böhm M, Kremer J and Louis A K 1993 Efficient algorithm for computing optimal control of antennas in hyperthermia *Surv. Math. Ind* **3** 233–251

Bornemann F, Erdmann B and Kornhuber R 1993 Adaptive Multilevel Methods in Three Space Dimensions *Int. J. Numer. Meth. Eng.* **36** 3187–3202

Deuflhard P, Leinen P and Yserentant H 1989 Concepts of an Adaptive Hierarchical Finite Elemet Code *IMPACT Comp. Sci. Eng.* **1** 3–35

Gellermann J, Wust P, Stalling D, Seebass M, Nadobny J, Beck R, Beier J, Hege H C, Deuflhard P and Felix R 1999 Clinical evaluation and verification of the hyperthermia treatment planning system HyperPlan *Int. J. Radiat. Oncol. Biol. Phys.* **47** 1145–1156

Köhler T 1999 Effiziente Algorithmen für die Optimierung der Therapie-Planung zur regionalen Hyperthermie (PhD–Thesis, Universität Potsdam)

Kremer J and Louis A K 1990 On the mathematical foundation of hyperthermia treatment *Math. Meth. Appl. Sci.* **13** 467–479

Lang L, Erdmann B and Seebass M 1997 Impact of Nonlinear heat Transfer on Temperature Control in Regional Hyperthermia (Berlin: Konrad–Zuse–Zentrum für Informationstechnik, Preprint SC 97-73)

Nadobny J, Sullivan D, Wust P, Seebass M, Deuflhard P and Felix R 1998 A High-Resolution Interpolation at Arbitrary Interfaces for the FDTD Method *IEEE Trans. Microwave Theory Tech.* **46** 1759–1766

Nikita K S, Maratos N G and Uzunoglu N K 1993 Optimal Steady-State Temperature Distribution for a Phased Array Hyperthermia System *IEEE Trans. on Biomed. Eng.* **40** 1299–1306

Rau B, Wust P, Tilly W, Gellermann J, Harder C, Riess H, Budach V, Felix R and Schlag M D 2000 Preoperative radiochemotherapy in locally rectal cancer: Regional radiofrequency hyperthermia correlates with clinical parameters *Int. J. Radiation Oncololgy Biol. Phys.* **48** 381–391

Roemer R B 1995 Inverse Techniques for Estimating Complete Temperature Distributions during Hyperthermia Cancer Therapy (Poitiers: French Heat Transfer Society (SFT) National Conference)

Wloderczyk W, Boroschewski R, Hentschel M, Wust P, Mönich G and Felix R 1998 Three-Dimensional Monitoring of Small Temperature Changes for Therapeutic Hyperthermia Using MR *J. Magn. Reson. Imag.* **8** 165–174

Wloderczyk W, Hentschel M, Wust P, Noeske R, Hosten N, Rinneberg H and Felix R 1999 Comparison of four magnetic resonance methods for mapping small temperature changes *Phys. Med. Biol.* **44** 607–624

Wust P, Berger J, Fähling H, Nadobny J, Gellermann J, Tilly W, Rau B, Petermann K and Felix R 1999a Scanning E-field sensor device for on-line control of annular-phased-array systems *Int. J. Radiat. Oncol. Biol. Phys.* **143** 927–937

Wust P, Nadobny J, Seebass M, Stalling D, Gellermann J, Hege H C, Deuflhard P and Felix R 1999b Influence of patient models and numerical methods on predicted power deposition patterns *Int. J. Hyperthermia* **15** 519–540

Wust P, Seebass M, Nadobny J, Deuflhard P, Mönich G and Felix R 1996 Simulation studies promote technological development of radiofrequency phased array hyperthermia *Int. J. Hyperthermia* **12** 477–494

**Berichte aus der Technomathematik** ISSN 1435-7968

http://www.math.uni-bremen.de/zetem/berichte.html

— Vertrieb durch den Autor —

**Reports** **Stand: 5. März 2001**

98–01. Peter Benner, Heike Faßbender:
*An Implicitly Restarted Symplectic Lanczos Method for the Symplectic Eigenvalue Problem*, Juli 1998.

98–02. Heike Faßbender:
*Sliding Window Schemes for Discrete Least-Squares Approximation by Trigonometric Polynomials*, Juli 1998.

98–03. Peter Benner, Maribel Castillo, Enrique S. Quintana-Ortí:
*Parallel Partial Stabilizing Algorithms for Large Linear Control Systems*, Juli 1998.

98–04. Peter Benner:
*Computational Methods for Linear–Quadratic Optimization*, August 1998.

98–05. Peter Benner, Ralph Byers, Enrique S. Quintana-Ortí, Gregorio Quintana-Ortí:
*Solving Algebraic Riccati Equations on Parallel Computers Using Newton's Method with Exact Line Search*, August 1998.

98–06. Lars Grüne, Fabian Wirth:
*On the rate of convergence of infinite horizon discounted optimal value functions*, November 1998.

98–07. Peter Benner, Volker Mehrmann, Hongguo Xu:
*A Note on the Numerical Solution of Complex Hamiltonian and Skew-Hamiltonian Eigenvalue Problems*, November 1998.

98–08. Eberhard Bänsch, Burkhard Höhn:
*Numerical simulation of a silicon floating zone with a free capillary surface*, Dezember 1998.

99–01. Heike Faßbender:
*The Parameterized SR Algorithm for Symplectic (Butterfly) Matrices*, Februar 1999.

99–02. Heike Faßbender:
*Error Analysis of the symplectic Lanczos Method for the symplectic Eigenvalue Problem*, März 1999.

99–03. Eberhard Bänsch, Alfred Schmidt:
*Simulation of dendritic crystal growth with thermal convection*, März 1999.

99–04. Eberhard Bänsch:
*Finite element discretization of the Navier-Stokes equations with a free capillary surface*, März 1999.

99–05. Peter Benner:
*Mathematik in der Berufspraxis*, Juli 1999.

99–06. Andrew D.B. Paice, Fabian R. Wirth:
*Robustness of nonlinear systems and their domains of attraction*, August 1999.

99–07. Peter Benner, Enrique S. Quintana-Ortí, Gregorio Quintana-Ortí:
*Balanced Truncation Model Reduction of Large-Scale Dense Systems on Parallel Computers*, September 1999.

99–08. Ronald Stöver:
*Collocation methods for solving linear differential-algebraic boundary value problems*, September 1999.

99–09. Huseyin Akcay:
*Modelling with Orthonormal Basis Functions*, September 1999.

99–10. Heike Faßbender, D. Steven Mackey, Niloufer Mackey:
*Hamilton and Jacobi come full circle: Jacobi algorithms for structured Hamiltonian eigenproblems*, Oktober 1999.

99–11. Peter Benner, Vincente Hernández, Antonio Pastor:
*On the Kleinman Iteration for Nonstabilizable System*, Oktober 1999.

99–12. Peter Benner, Heike Faßbender:
*A Hybrid Method for the Numerical Solution of Discrete-Time Algebraic Riccati Equations*, November 1999.

99–13. Peter Benner, Enrique S. Quintana-Ortí, Gregorio Quintana-Ortí:
*Numerical Solution of Schur Stable Linear Matrix Equations on Multicomputers*, November 1999.

99–14. Eberhard Bänsch, Karol Mikula:
*Adaptivity in 3D Image Processing*, Dezember 1999.

00–01. Peter Benner, Volker Mehrmann, Hongguo Xu:
*Perturbation Analysis for the Eigenvalue Problem of a Formal Product of Matrices*, Januar 2000.

00–02. Ziping Huang:
*Finite Element Method for Mixed Problems with Penalty*, Januar 2000.

00–03. Gianfrancesco Martinico:
*Recursive mesh refinement in 3D*, Februar 2000.

00–04. Eberhard Bänsch, Christoph Egbers, Oliver Meincke, Nicoleta Scurtu:
*Taylor-Couette System with Asymmetric Boundary Conditions*, Februar 2000.

00–05. Peter Benner:
*Symplectic Balancing of Hamiltonian Matrices*, Februar 2000.

00–06. Fabio Camilli, Lars Grüne, Fabian Wirth:
*A regularization of Zubov's equation for robust domains of attraction*, März 2000.

00–07. Michael Wolff, Eberhard Bänsch, Michael Böhm, Dominic Davis:
*Modellierung der Abkühlung von Stahlbrammen*, März 2000.

00–08. Stephan Dahlke, Peter Maaß, Gerd Teschke:
*Interpolating Scaling Functions with Duals*, April 2000.

00–09. Jochen Behrens, Fabian Wirth:
*A globalization procedure for locally stabilizing controllers*, Mai 2000.

00–10. Peter Maaß, Gerd Teschke, Werner Willmann, Günter Wollmann:
*Detection and Classification of Material Attributes – A Practical Application of Wavelet Analysis*, Mai 2000.

00–11. Stefan Boschert, Alfred Schmidt, Kunibert G. Siebert, Eberhard Bänsch, Klaus-Werner Benz, Gerhard Dziuk, Thomas Kaiser:
*Simulation of Industrial Crystal Growth by the Vertical Bridgman Method*, Mai 2000.

00–12. Volker Lehmann, Gerd Teschke:
*Wavelet Based Methods for Improved Wind Profiler Signal Processing*, Mai 2000.

00–13. Stephan Dahlke, Peter Maass:
*A Note on Interpolating Scaling Functions*, August 2000.

00–14. Ronny Ramlau, Rolf Clackdoyle, Frédéric Noo, Girish Bal:
*Accurate Attenuation Correction in SPECT Imaging using Optimization of Bilinear Functions and Assuming an Unknown Spatially-Varying Attenuation Distribution*, September 2000.

00–15. Peter Kunkel, Ronald Stöver:
*Symmetric collocation methods for linear differential-algebraic boundary value problems*, September 2000.

00–16. Fabian Wirth:
*The generalized spectral radius and extremal norms*, Oktober 2000.

00–17. Frank Stenger, Ahmad Reza Naghsh-Nilchi, Jenny Niebsch, Ronny Ramlau:
*A unified approach to the approximate solution of PDE*, November 2000.

00–18. Peter Benner, Enrique S. Quintana-Ortí, Gregorio Quintana-Ortí:
*Parallel algorithms for model reduction of discrete–time systems*, Dezember 2000.

00–19. Ronny Ramlau:
*A steepest descent algorithm for the global minimization of Tikhonov–Phillips functional*, Dezember 2000.

01–01. Efficient methods in hyperthermia treatment planning:
*Torsten Köhler, Peter Maass, Peter Wust, Martin Seebass*, Januar 2001.

01–02. Parallel Algorithms for LQ Optimal Control of Discrete-Time Periodic Linear Systems:
*Peter Benner, Ralph Byers, Rafael Mayo, Enrique S. Quintana-Ortí, Vicente Hernández*, Februar 2001.

01–03. Peter Benner, Enrique S. Quintana-Ortí, Gregorio Quintana-Ortí:
*Efficient Numerical Algorithms for Balanced Stochastic Truncation*, März 2001.